

# Localized Charged-Neutral Fluctuations in 158 A GeV Pb+Pb Collisions

M.M. Aggarwal,<sup>1</sup> A. Agnihotri,<sup>2</sup> Z. Ahammed,<sup>3</sup> A.L.S. Angelis,<sup>4</sup> V. Antonenko,<sup>5</sup> V. Arefiev,<sup>6</sup> V. Astakhov,<sup>6</sup> V. Avdeitchikov,<sup>6</sup> T.C. Awes,<sup>7</sup> P.V.K.S. Baba,<sup>8</sup> S.K. Badyal,<sup>8</sup> C. Barlag,<sup>9</sup> S. Bathe,<sup>9</sup> B. Batiounia,<sup>6</sup> T. Bernier,<sup>10</sup> K.B. Bhalla,<sup>2</sup> V.S. Bhatia,<sup>1</sup> C. Blume,<sup>9</sup> R. Bock,<sup>11</sup> E.-M. Bohne,<sup>9</sup> Z. Bőröcz,<sup>9</sup> D. Bucher,<sup>9</sup> A. Buijs,<sup>12</sup> H. Büsching,<sup>9</sup> L. Carlen,<sup>13</sup> V. Chalyshev,<sup>6</sup> S. Chattopadhyay,<sup>3</sup> R. Cherbatchev,<sup>5</sup> T. Chujo,<sup>14</sup> A. Claussen,<sup>9</sup> A.C. Das,<sup>3</sup> M.P. Decowski,<sup>18</sup> H. Delagrange,<sup>10</sup> V. Djordjadze,<sup>6</sup> P. Donni,<sup>4</sup> I. Doubovik,<sup>5</sup> A.K. Dubey,<sup>19</sup> S. Dutt,<sup>8</sup> M.R. Dutta Majumdar,<sup>3</sup> K. El Chenawi,<sup>13</sup> S. Eliseev,<sup>15</sup> K. Enosawa,<sup>14</sup> P. Foka,<sup>4</sup> S. Fokin,<sup>5</sup> M.S. Ganti,<sup>3</sup> S. Garpman,<sup>13</sup> O. Gavrishchuk,<sup>6</sup> F.J.M. Geurts,<sup>12</sup> T.K. Ghosh,<sup>16</sup> R. Glasow,<sup>9</sup> S. K. Gupta,<sup>2</sup> B. Guskov,<sup>6</sup> H. Å.Gustafsson,<sup>13</sup> H. H.Gutbrod,<sup>10</sup> R. Higuchi,<sup>14</sup> I. Hrivnacova,<sup>15</sup> M. Ippolitov,<sup>5</sup> H. Kalechofsky,<sup>4</sup> R. Kamermans,<sup>12</sup> K.-H. Kampert,<sup>9</sup> K. Karadjev,<sup>5</sup> K. Karpio,<sup>17</sup> S. Kato,<sup>14</sup> S. Kees,<sup>9</sup> C. Klein-Bösing,<sup>9</sup> S. Knoche,<sup>9</sup> B. W. Kolb,<sup>11</sup> I. Kosarev,<sup>6</sup> I. Koutcheryaev,<sup>5</sup> T. Krümpel,<sup>9</sup> A. Kugler,<sup>15</sup> P. Kulinich,<sup>18</sup> M. Kurata,<sup>14</sup> K. Kurita,<sup>14</sup> N. Kuzmin,<sup>6</sup> I. Langbein,<sup>11</sup> A. Lebedev,<sup>5</sup> Y.Y. Lee,<sup>11</sup> H. Löhner,<sup>16</sup> L. Luquin,<sup>10</sup> D.P. Mahapatra,<sup>19</sup> V. Manko,<sup>5</sup> M. Martin,<sup>4</sup> G. Martínez,<sup>10</sup> A. Maximov,<sup>6</sup> G. Mgebrichvili,<sup>5</sup> Y. Miake,<sup>14</sup> Md.F. Mir,<sup>8</sup> G.C. Mishra,<sup>19</sup> Y. Miyamoto,<sup>14</sup> B. Mohanty,<sup>19</sup> M.-J. Mora,<sup>10</sup> D. Morrison,<sup>20</sup> D. S. Mukhopadhyay,<sup>3</sup> H. Naef,<sup>4</sup> B. K. Nandi,<sup>19</sup> S. K. Nayak,<sup>10</sup> T. K. Nayak,<sup>3</sup> S. Neumaier,<sup>11</sup> A. Nianine,<sup>5</sup> V. Nikitine,<sup>6</sup> S. Nikolaev,<sup>13</sup> P. Nilsson,<sup>13</sup> S. Nishimura,<sup>14</sup> P. Nomokonov,<sup>6</sup> J. Nystrand,<sup>13</sup> F.E. Obenshain,<sup>20</sup> A. Oskarsson,<sup>13</sup> I. Otterlund,<sup>13</sup> M. Pachr,<sup>15</sup> S. Pavliouk,<sup>6</sup> T. Peitzmann,<sup>9</sup> V. Petracek,<sup>15</sup> W. Pinganaud,<sup>10</sup> F. Plasil,<sup>7</sup> U. v. Poblitzki,<sup>9</sup> M.L. Purschke,<sup>11</sup> J. Rak,<sup>15</sup> R. Raniwala,<sup>2</sup> S. Raniwala,<sup>2</sup> V.S. Ramamurthy,<sup>19</sup> N.K. Rao,<sup>8</sup> F. Retiere,<sup>10</sup> K. Reygers,<sup>9</sup> G. Roland,<sup>18</sup> L. Rosselet,<sup>4</sup> I. Roufanov,<sup>6</sup> C. Roy,<sup>10</sup> J.M. Rubio,<sup>4</sup> H. Sako,<sup>14</sup> S.S. Sambyal,<sup>8</sup> R. Santo,<sup>9</sup> S. Sato,<sup>14</sup> H. Schlagheck,<sup>9</sup> H.-R. Schmidt,<sup>11</sup> Y. Schutz,<sup>10</sup> G. Shabratova,<sup>6</sup> T.H. Shah,<sup>8</sup> I. Sibiriak,<sup>5</sup> T. Siemiarczuk,<sup>17</sup> D. Silvermyr,<sup>13</sup> B.C. Sinha,<sup>3</sup> N. Slavine,<sup>6</sup> K. Söderström,<sup>13</sup> N. Solomey,<sup>4</sup> G. Sood,<sup>1</sup> S.P. Sørensen,<sup>7,20</sup> P. Stankus,<sup>7</sup> G. Stefanek,<sup>17</sup> P. Steinberg,<sup>18</sup> E. Stenlund,<sup>13</sup> D. Stüken,<sup>9</sup> M. Sumera,<sup>15</sup> T. Svensson,<sup>13</sup> M.D. Trivedi,<sup>3</sup> A. Tsvetkov,<sup>5</sup> L. Tykarski,<sup>17</sup> J. Urbahn,<sup>11</sup> E.C.v.d. Pijll,<sup>12</sup> N.v. Eijndhoven,<sup>12</sup> G.J.v. Nieuwenhuizen,<sup>18</sup> A. Vinogradov,<sup>5</sup> Y.P. Viyogi,<sup>3</sup> A. Vodopianov,<sup>6</sup> S. Vörös,<sup>4</sup> B. Wysłouch,<sup>18</sup> K. Yagi,<sup>14</sup> Y. Yokota,<sup>14</sup> G.R. Young<sup>7</sup>

(WA98 Collaboration)

<sup>1</sup> University of Panjab, Chandigarh 160014, India

<sup>2</sup> University of Rajasthan, Jaipur 302004, Rajasthan, India

<sup>3</sup> Variable Energy Cyclotron Centre, Calcutta 700 064, India

<sup>4</sup> University of Geneva, CH-1211 Geneva 4, Switzerland

<sup>5</sup> RRC "Kurchatov Institute", RU-123182 Moscow, Russia

<sup>6</sup> Joint Institute for Nuclear Research, RU-141980 Dubna, Russia

<sup>7</sup> Oak Ridge National Laboratory, Oak Ridge, Tennessee 37831-6372, USA

<sup>8</sup> University of Jammu, Jammu 180001, India

<sup>9</sup> University of Münster, D-48149 Münster, Germany

<sup>10</sup> SUBATECH, Ecole des Mines, Nantes, France

<sup>11</sup> Gesellschaft für Schwerionenforschung (GSI), D-64220 Darmstadt, Germany

<sup>12</sup> Universiteit Utrecht/NIKHEF, NL-3508 TA Utrecht, The Netherlands

<sup>13</sup> University of Lund, SE-221 00 Lund, Sweden

<sup>14</sup> University of Tsukuba, Ibaraki 305, Japan

<sup>15</sup> Nuclear Physics Institute, CZ-250 68 Rez, Czech Rep.

<sup>16</sup> KVI, University of Groningen, NL-9747 AA Groningen, The Netherlands

<sup>17</sup> Institute for Nuclear Studies, 00-681 Warsaw, Poland

<sup>18</sup> MIT Cambridge, MA 02139, USA

<sup>19</sup> Institute of Physics, 751-005 Bhubaneswar, India

<sup>20</sup> University of Tennessee, Knoxville, Tennessee 37966, USA

(Draft 5.0, October 29, 2018)

First results on the measurement of localized fluctuations in the multiplicity of charged particles and photons produced in central 158-A GeV/c Pb+Pb collisions are presented. The charged versus neutral correlations in common phase space regions of varying azimuthal size are analyzed by two different methods. The measured results are compared to those from simulations and to those from different types of mixed events. The comparison indicates the presence of non-statistical fluctuations in both charged particle and photon multiplicities in limited azimuthal regions. However, no correlated charge-neutral fluctuations are observed.

25.75.+r,13.40.-f,24.90.+p

The formation of hot and dense matter in high energy heavy-ion collisions offers the possibility to create a new phase where matter is deconfined and chiral symmetry is restored. Indications for the formation of such a Quark Gluon Plasma (QGP) phase are provided by several results from experiments at the CERN-SPS [1]. Event-by-event fluctuations in the particle multiplicities and their ratios have recently been predicted to provide information about the nature of the QCD phase transition [2,3]. Fluctuations may also be caused by Bose-Einstein correlations, resonance decays, or more exotic phenomena such as pion lasers [4]. Enhanced fluctuations in neutral to charged pions have been predicted as a signature of the formation of disoriented chiral condensates (DCC) [5–8], which might be one of the most interesting predicted consequences of chiral symmetry restoration.

Theoretical predictions suggest that isospin fluctuations, caused by formation of a DCC, would produce clusters of coherent pions in localized phase space regions or domains. The probability distribution of the neutral pion fraction in such a domain would follow the relation  $P(f) = 1/2\sqrt{f}$ , where  $f = N_{\pi^0}/N_{\pi}$ . Thus DCC formation in a given domain would be associated with large event-by-event fluctuations in the ratio of neutral to charged pions in that domain. Experimentally, such fluctuations can be deduced from the measurement of fluctuations in the number of photons to charged particles in limited  $\eta$ - $\phi$  regions. The anti-Centauro events, reported by the JACEE collaboration [9], with large charged-neutral fluctuations are possible candidates for DCC events. The studies carried out so far in  $p - \bar{p}$  [10] and heavy ion [11,12] reactions have searched for fluctuations which extend over a large region of phase space. These measurements have provided upper limits on the presence of DCC-like fluctuations.

In this letter we present first results on the search for non-statistical event-by-event fluctuations in the relative number of charged particles and photons in localized phase space regions for central 158-A GeV/c Pb+Pb collisions. The data presented here were taken with the 158-A GeV Pb beam of the CERN SPS on a Pb target of 213  $\mu\text{m}$  thickness during a period of WA98 operation without magnetic field. The analysis makes use of a subset of detectors of the WA98 experiment which are used to measure the multiplicities of charged particles and photons. Charged particle hits ( $N_{\text{ch}}$ ) were counted using a circular Silicon Pad Multiplicity Detector (SPMD) [11] located 32.8 cm downstream from the target. It provided uniform pseudorapidity coverage in the region  $2.35 < \eta < 3.75$ . The detector was 99% efficient for charged particle detection. The photon multiplicity was measured using a preshower Photon Multiplicity Detector (PMD) [13] placed 21.5 meters downstream of the target and covering the pseudorapidity range  $2.9 < \eta < 4.2$ . It consisted of an array of 53,200 plastic scintillator pads placed behind  $3X_0$  thick lead converter plates. Clusters of hit pads having total energy deposit above a hadron rejection threshold are identified as photon-like. The photon counting efficiency and the purity of the  $\gamma$ -like sample have been found to be 68% and 65%, respectively, for central events [14]. For this analysis the pseudorapidity region

of common coverage of the SPMD and PMD was selected ( $2.9 < \eta < 3.75$ ). The acceptance in terms of transverse momentum ( $p_T$ ) extends down to 30 MeV/c, although no explicit  $p_T$ -selection is applied. Events with pile-up or downstream interactions were rejected in the off-line analysis. Strict data selection and cleanup cuts have been applied as described in Ref. [11,14]. After cuts, a total of 85K central events, corresponding to the top 5% of the minimum bias cross section as determined from the measured total transverse energy, have been analyzed.

The measured results are interpreted by comparison with simulated events and with several types of mixed events. Simulated events were generated using the VENUS 4.12 [15] event generator with default parameters. The output was processed through a WA98 detector simulation package in the GEANT 3.21 [16] framework. The centrality selection for the simulated data has been made in an identical manner to the experimental data by selection on the simulated total transverse energy in the WA98 acceptance. The simulated VENUS+GEANT events (referred as V+G) were then processed with the same analysis codes as used for the analysis of the experimental data.

The effect of non-statistical DCC-like charged-neutral fluctuations has been studied within the framework of a simple model in which the output of the VENUS event generator has been modified. It is expected that DCC domains will occur in small regions and will mostly modify the production of low momentum pions. The influence of a DCC on the charge-neutral pion ratio may then be limited to localized  $\eta$ - $\phi$  regions due to the motion of the DCC domain within the overall collective motion. To implement the DCC effect, the charges of the pions within a localized  $\eta$ - $\phi$  region predicted by VENUS are interchanged pairwise ( $\pi^+\pi^- \leftrightarrow \pi^0\pi^0$ ) according to the  $1/2\sqrt{f}$  probability distribution. The DCC-like fluctuations were generated over  $\eta = 3 - 4$  for varying intervals in  $\Delta\phi$ . Since the probability to produce events with DCC domains is unknown, ensembles of events, here referred to as a “nDCC events”, were produced which consisted of a mixture of normal events with varying fractions of pure DCC-like events. The nDCC events were then tracked through GEANT.

In the search for evidence of non-statistical charged-neutral fluctuations, two different analysis techniques have been applied. The first method employed in the present analysis is the technique of discrete wavelet transformations (DWT). DWT methods are now widely used in many applications, such as data compression and image processing, and have been shown to provide a powerful means to search for localized domains of DCC [17,18]. While there are several families of wavelet bases distinguished by the number of coefficients and the level of iteration, we have used the frequently employed  $D=4$  wavelet basis [20], which are orthogonal, continuously differentiable and localized in space. The analysis has been performed with the sample function chosen to be the photon fraction, given by  $f'(\phi) = N_{\gamma\text{-like}}(\phi)/(N_{\gamma\text{-like}}(\phi) + N_{\text{ch}}(\phi))$  as a function of the azimuthal angle  $\phi$ , with highest resolution scale  $j_{\text{max}} = 5$ . The input to the DWT analysis is the

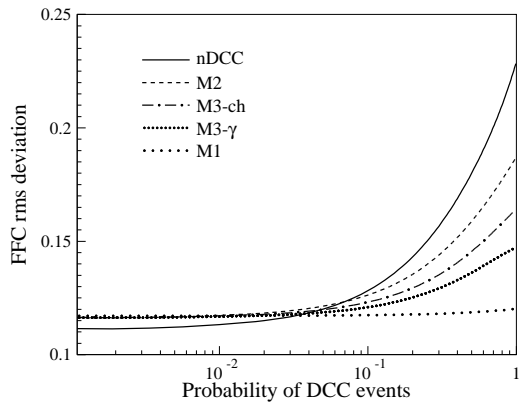


FIG. 1. The rms deviations of the FFC distributions at  $j = 1$  for simulated nDCC events with extent  $\Delta\phi_{DCC} = 90^\circ$  and for various mixed events constructed from those events, as a function of the fraction of DCC-like events present in the nDCC sample.

spectrum of the sample function at the smallest bin size corresponding to the highest resolution scale,  $j_{max}$ , where the number of bins is  $2^{j_{max}}$ . The sample function is then analyzed at different scales  $j$  by being re-binned into  $2^j$  bins. The DWT analysis yields a set of wavelets or father function coefficients (FFC) at each scale from  $j = 1, \dots, (j_{max} - 1)$ . The coefficients obtained at a given scale,  $j$ , are derived from the distribution of the sample function at one higher scale,  $j + 1$ . The FFCs quantify the deviation of the bin-to-bin fluctuations in the sample function at that higher scale relative to the average behavior. The presence of localized non-statistical fluctuations will increase the rms deviation of the distribution of FFCs and may result in non-Gaussian tails [17,18].

The DWT technique as used in this analysis is demonstrated in Fig. 1 where it has been applied to the simulated nDCC events. The rms deviation of the FFC distribution is shown as a function of the fraction of DCC-like events in the nDCC sample. The rms deviation is observed to increase strongly with increasing DCC-like fraction. Due to the inherent uncertainties in the description of “normal” physics and detector response in the V+G simulations, the observation of an experimental result with rms which differs from the case with zero DCC fraction cannot be taken alone as evidence of DCC observation. For this reason four different types of mixed events have been created from the real or simulated events in order to search for non-statistical fluctuations by removing various correlations in a controlled manner while preserving the characteristics of the measured distributions as accurately as possible. The first type of mixed events (M1), are generated by mixing hits in both the PMD and SPMD separately, with no two hits taken from the same event. Hits within a detector in the mixed events are not allowed to lie within the two track resolution of that detector. The second kind of mixed events (M2) are generated by mixing the unaltered PMD hits of one event with the unaltered SPMD hits of a different event. Intermediate between the M1 and M2 kinds of mixed events is the case where the hits within the PMD are unaltered while

the SPMD hits are mixed (M3- $\gamma$ ), or the SPMD hits are unaltered while the PMD hits are mixed (M3-ch). In each type of mixed event the global (bin 1)  $N_{\gamma\text{-like}}-N_{ch}$  correlation is maintained as in the real event.

The rms deviations of the FFCs for the different kinds of mixed events produced from the nDCC events are also shown in Fig. 1. In the case of vanishing DCC-like fluctuations, the rms values of the various types of mixed events are very close to each other. The V+G rms values are lower than those of the mixed events due to the presence of additional correlations between  $N_{ch}$  and  $N_{\gamma\text{-like}}$  mostly as a result of the charged particle contamination in the  $N_{\gamma\text{-like}}$  sample. The rms deviations for the M1 events are found to be almost independent of probability of DCC-like events, while the rms deviations of the M2 events increase similarly, but more weakly, than those of the nDCC events. The rms deviations for the M3 sets of events are found to lie between M2 and M1. Thus, the sequence of the mixed events relative to the simulated events (or data) gives a model independent indication of the presence and source of non-statistical fluctuations. The simple DCC model used here results in an anti-correlation between  $N_{\gamma\text{-like}}$  and  $N_{ch}$  due to the “isospin-flip” procedure used to implement the DCC effect. It also results in non-statistical fluctuations in both  $N_{\gamma\text{-like}}$  and  $N_{ch}$ . Thus the M2 events remove only the  $N_{\gamma\text{-like}}-N_{ch}$  anti-correlation while the M1 events are seen to remove all non-statistical fluctuations and correlations. The M3 mixed events give intermediate results because they contain only the  $N_{\gamma\text{-like}}$  (M3- $\gamma$ ) or  $N_{ch}$  (M3-ch) non-statistical fluctuations.

The FFC distributions extracted from the measured  $f'(\phi)$  ratio are shown in the bottom panel of Fig. 2 for the experimental data, for M1 events (from data), and for V+G events. The results are shown for scales  $j = 1$  and 2, which carry information about fluctuations at  $90^\circ$  and  $45^\circ$  in  $\phi$ . The FFC distributions of the experimental distributions are seen to be broader than the V+G and M1 results. This suggests the presence of non-statistical fluctuations.

A more conventional method similar to that described in Ref. [11] has also been used to search for non-statistical fluctuations. The correlation between  $N_{\gamma\text{-like}}$  and  $N_{ch}$  has been studied in varying  $\phi$  intervals, by dividing the entire  $\phi$ -space into 2, 4, 8, and 16 bins. The correlation plot of  $N_{ch}$  versus  $N_{\gamma\text{-like}}$  [19] is obtained for each  $\phi$  segmentation, starting with the case of 1 bin which corresponds to the full azimuth. A common correlation axis ( $Z$ ) has been obtained for the full distribution by fitting the mean  $N_{\gamma\text{-like}}$  and  $N_{ch}$  values with a second order polynomial. The distance of separation ( $D_Z$ ) between the data points and the correlation axis has been calculated with the convention that  $D_Z$  is positive for points below the  $Z$ -axis (increasing  $N_{\gamma\text{-like}}$ ). The distribution of  $D_Z$  represents the fluctuations of  $N_{\gamma\text{-like}}$  relative to  $N_{ch}$  compared to the common correlation axis. In order to compare fluctuations at different bin sizes having different multiplicities we use a scaled variable,  $S_Z = D_Z/s(D_Z)$ , where  $s(D_Z)$  is the rms deviation of the  $D_Z$  distributions for V+G events. The presence of events with localized non-statistical fluctuations

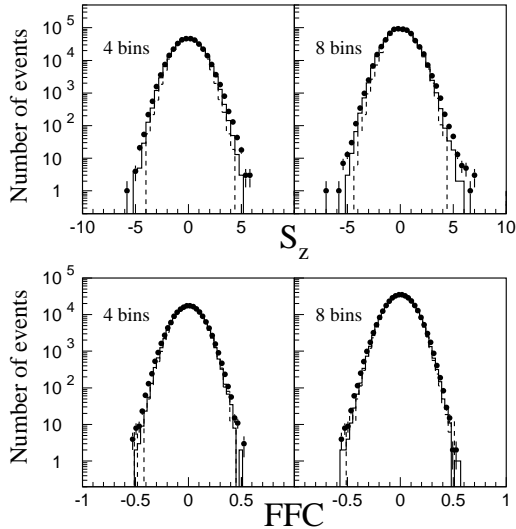


FIG. 2. The  $S_Z$  and FFC distributions for 4 and 8 divisions in  $\phi$ . The experimental data, M1 and V+G events are shown by solid circles, solid histograms and dashed histograms, respectively. The statistics for data and mixed events are same, whereas the distribution for the V+G events is normalized to the number of data events.

would be expected to result in a broader distribution of  $S_Z$  compared to those for normal events. The  $S_Z$  distributions calculated at 4 and 8 bins in  $\phi$  angle are shown in the top panel of Fig. 2 for data, M1, and V+G events. The experimental distributions are broader than the simulation and M1 results, again indicating the presence of additional fluctuations.

The rms deviations of the  $S_Z$  and FFC distributions as a function of the number of bins in azimuth is shown for experimental data, mixed events, and V+G in Fig. 3. The statistical errors on the values are small and lie within the size of the symbols. The error bars include both statistical and systematic errors. The systematic errors have been estimated by investigation of effects such as the uncertainties in the detection efficiencies, gain fluctuations, backgrounds, binning variations, and fitting procedures. Since the mixed events are constructed to maintain the  $N_{\gamma\text{-like}}-N_{\text{ch}}$  correlations for the full azimuth (bin 1), the rms deviations of data and mixed events for this bin are identical. The difference of the  $S_Z$  rms deviations between data and V+G for this bin is the same as reported in an earlier WA98 publication [11]. The comparison of V+G and the M1 mixed events demonstrates the utility of the DWT method to normalize out the average behavior when the bin-to-bin fluctuation information is extracted.

As noted in the discussion of Fig. 1, even in the absence of DCCs there exist uninteresting correlations between  $N_{\gamma\text{-like}}$  and  $N_{\text{ch}}$  which are removed by the event mixing procedure and thereby result in a difference between the real and mixed events. The various mixed event rms values of Fig. 3 have therefore been rescaled by the percentage difference between the rms deviations of the V+G distributions and those of the corresponding V+G mixed events in order to better illustrate

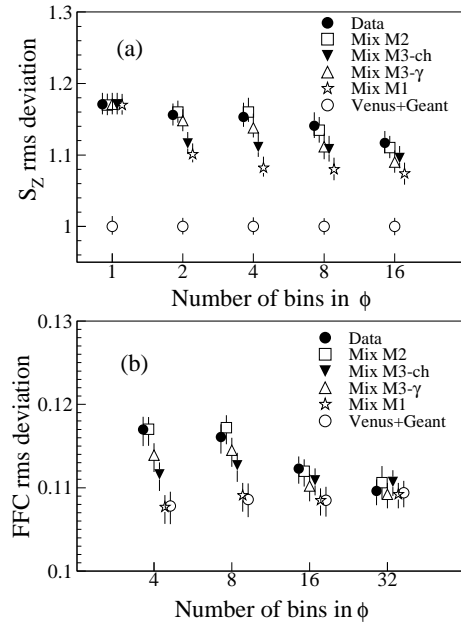


FIG. 3. The root mean square (rms) deviations of the  $S_Z$  and FFC distributions for various divisions in the azimuthal angle.

effects in the data beyond those present in V+G. Taking the larger of the asymmetric systematic error at each point to be one sigma, we find that at 2, 4, and 8 bins the values of the  $S_Z$  rms deviations of the data are  $3.2\sigma$ ,  $3.4\sigma$ , and  $3.1\sigma$  larger than those of M1 events, respectively. Similarly, the FFC rms deviations at 4 and 8 bins for data are  $4.3\sigma$  and  $3.3\sigma$  larger than those of the M1 events. At 16 and 32 bins, the result for mixed events and data agree within the quoted errors. The corrected rms deviations of the M2 events agree with those of the experimental data within error for all bins. The M3 type mixed events are found to be similar to each other within the quoted errors and lie between M1 and M2.

The observation that the rms deviations of the  $S_Z$  and FFC distributions for experimental data are larger than those of the M1 events indicates the presence of localized non-statistical fluctuations. However, the comparison of the rms deviations for data with those of M2 events implies the absence of event-by-event correlated fluctuations in  $N_{\gamma\text{-like}}$  versus  $N_{\text{ch}}$ . The M3-type mixed events indicate the presence of localized independent fluctuations in  $N_{\gamma\text{-like}}$  and  $N_{\text{ch}}$  of similar magnitude.

If the amount of DCC-like fluctuations in the experimental data were large, then the rms deviations shown in Fig. 3 for data would have been larger compared to those of M2 events. Since this is not the case, we compare the measured results with those obtained from the simulation as shown in Fig. 1 to extract upper limits on the probability of DCC-like fluctuations at the 90% confidence level. Within the context of this simple DCC model, upper limits on the presence of localized non-statistical DCC-like fluctuations of  $10^{-2}$  for  $\Delta\phi$  between  $45^\circ$ - $90^\circ$  and  $3 \times 10^{-3}$  for  $\Delta\phi$  between  $90^\circ$ - $135^\circ$  are extracted.

In summary, a detailed event-by-event analysis of the fluctuations in the  $\eta - \phi$  phase space distributions of charged

particles and photons has been performed for central Pb+Pb collisions at 158-A GeV using two complementary analysis methods. The first analysis employed the discrete wavelet transformation technique to investigate the relative magnitude of the  $N_{\gamma\text{-like}}$  versus  $N_{\text{ch}}$  fluctuations in adjacent phase space regions. The second method studied the magnitude of the  $N_{\gamma\text{-like}}$  versus  $N_{\text{ch}}$  multiplicity fluctuations in decreasing phase space regions. The results were compared to pure VENUS+GEANT simulations and to various types of mixed events to isolate the source of non-statistical fluctuations. Both analysis methods indicated non-statistical fluctuations beyond simulation and beyond pure mixed events at the 3-4 $\sigma$  level for  $\phi$  intervals of greater than 45°. This is found to be due to uncorrelated non-statistical fluctuations in  $N_{\gamma\text{-like}}$  and  $N_{\text{ch}}$ . No significant correlated fluctuations in  $N_{\gamma\text{-like}}$  versus  $N_{\text{ch}}$  were observed. The results allow to set an upper limit on the frequency of production of DCCs of limited domain size, as demonstrated with a simple model of DCC-like fluctuations.

We wish to express our gratitude to the CERN accelerator division for the excellent performance of the SPS accelerator complex. We acknowledge with appreciation the effort of all engineers, technicians and support staff who have participated in the construction of this experiment. This work was supported jointly by the German BMBF and DFG, the U.S. DOE, the Swedish NFR and FRN, the Dutch Stichting FOM, the Polish KBN under contract 621/E-78/SPUB/CERN/P-03/DZ211, the Grant Agency of the Czech Republic under contract No. 202/95/0217, the Department of Atomic Energy, the Department of Science and Technology, the Council of Scientific and Industrial Research and the University Grants Commission of the Government of India, the Indo-FRG Exchange Program, the PPE division of CERN, the Swiss National Fund, the INTAS under Contract INTAS-97-0158, ORISE, Grant-in-Aid for Scientific Research (Specially Promoted Research & International Scientific Research) of the Ministry of Education, Science and Culture, the University of Tsukuba Special Research Projects, and the JSPS Research Fellowships for Young Scientists. ORNL is managed by UT-Battelle, LLC, for the U.S. Department of Energy under contract DE-AC05-00OR22725. The MIT group has been supported by the US Dept. of Energy under the cooperative agreement DE-FC02-94ER40818.

- [7] J. -P. Blaizot and A. Krzywicki, Phys. Rev. D **46**, 246 (1992).
- [8] K. Rajagopal and F. Wilczek, Nucl. Phys. B **399**, 395 (1993); Nucl. Phys. B **404**, 577 (1993).
- [9] C.M.G. Lattes, et al., Phys. Rep. **65**, 151 (1980).
- [10] Minimax Collaboration, T.C. Brooks et al., Phys. Rev. D **61**, 032003 (2000).
- [11] WA98 Collaboration, M.M. Aggarwal et al., Phys. Lett. B **420**, 169 (1998).
- [12] NA49 Collaboration, H. Appelshauser et al., Phys. Lett. B **459**, 679 (1999).
- [13] M.M. Aggarwal et al., Nucl. Instr. and Meth. A **424**, 395 (1999).
- [14] WA98 Collaboration, M.M. Aggarwal et al., Phys. Lett. B **458**, 422 (1999).
- [15] K. Werner, Phys. Rep. **232**, 87 (1993).
- [16] R. Brun et al., GEANT3 user's guide, CERN/DD/EE/84-1 (1984).
- [17] Z. Huang, et al., Phys. Rev. D **54**, 750 (1996).
- [18] B.K. Nandi, et al., Phys. Lett. B **461**, 142 (1999).
- [19] WA98 Collaboration, B. Mohanty et al., Czech. Journal of Phys. Vol. **50-S2**, 126 (2000).
- [20] Numerical Recipes, Cambridge Univ. Press, 1998.

- 
- [1] See, for example, Proceedings of *Quark Matter '99*, Nucl. Phys. A **661** (1999).
  - [2] M. Stephanov, et al., Phys. Rev. Lett. **81**, 4816 (1998).
  - [3] M.Asakawa, U.Heinz, and B.Müller, Phys. Rev. Lett. **85**, 2072 (2000); S. Jeon and V. Koch, Phys. Rev. Lett. **85**, 2076 (2000).
  - [4] S. Pratt, Phys. Lett. B **301**, 159 (1993).
  - [5] A.A. Anselm, M.G. Ryskin, Phys. Lett. B **266**, 482 (1991).
  - [6] J.D. Bjorken, Int. J. Mod. Phys. A **7**, 4189 (1992).